

GLOBAL FLOW STABILITY ANALYSIS AND REDUCED ORDER MODELING FOR BLUFF-BODY FLOW CONTROL

MAREK MORZYŃSKI

*Poznan University of Technology, Institute of Combustion Engines and Transportation, Poland
e-mail: morzynski@stanton.ice.put.poznan.pl*

BERND R. NOACK

*Berlin University of Technology, Institute of Fluid Dynamics and Technical Acoustics, Germany
e-mail: bernd.r.noack@tu-berlin.de*

GILEAD TADMOR

*Northeastern University, Department of Electrical and Computer Engineering, Boston, USA
e-mail: tadmor@ece.neu.edu*

In the present study, a hierarchy of control-oriented reduced order models (ROMs) for fluid flows is presented. Control design requires simplicity, accuracy and robustness from an online capable Galerkin model. These requirements imply low order of the associated dynamical system. Standard POD (proper orthogonal decomposition) Galerkin models may provide a low-dimensional representation of a given reference state. Yet, their narrow dynamic range and lack of robustness pose a challenge for control design. We propose key enablers to increase the dynamic range of the POD model. An 11-dimensional hybrid model is discussed which includes, in addition to 8 POD modes, a shift mode to resolve base-flow variations, and a complex global stability mode for enhanced description of the transient phase. The dimension is further reduced by a similarly accurate 3-dimensional generalized mean-field model employing a novel continuous mode interpolation technique between POD and stability eigenmodes. This method connects smoothly different operating conditions, different mode bases and even different boundary conditions, allowing the design of least-order, accurate Galerkin model for flow control purposes. The interpolation technique is employed to construct *a priori* flow model from the stability analysis and the Reynolds equation without the need for flow data.

Key words: Reduced Order Models, control-oriented models, global flow stability, flow control, continuous mode interpolation

1. Introduction

Air-borne and ground transport systems are required to be more energy-efficient, targeting lower energy consumption and lower environmental pol-

lution. Flow control is one key enabler towards this target. These economic and environmental considerations emphasize practical flow control strategies as an important field of investigation (Fiedler and Fernholz, 1990; Gad-el-Hak, 2000). Such a strategy implies good choices of the type of actuator, its location, as well as its amplitude and frequency range. Hitherto, many practical actuation systems (acoustic actuator, winglets, ...) are obtained by engineering wisdom and understanding of the flow phenomena. Currently, the complexity of flows associated with transport systems require a more rigorous model-based hardware selection. An agreed set of best practices is still a distant target. Similar considerations apply even more so to sensing and control solutions.

Flow control may be operated in (i) passive (ii) active open-loop and (iii) active closed-loop mode. Passive control means are already a standard practice. Riblets used with the existing airplane configuration significantly reduce drag (Bechert *et al.*, 1997; Bechert and Hope, 1985). LEBUs (large-eddy-breakup devices), vortex generators, splitter plates, Strykowski wires, are among other passive means already implemented. Also active open-loop control has been investigated since many decades (Gad-el-Hak, 2000; Gad-el-Hak and Busnell, 1991; Lumley and Blossey, 1998; Smith and Baillieul, 2000; Wygnanski and Seifert, 1994). Synthetic jet actuation (Smith *et al.*, 1998) or plasma actuators (Kim *et al.*, 2005; Thomas *et al.*, 2006) enjoy an increasing popularity in experimental studies.

When compared with passive control and open-loop actuation, feedback control offers opportunities to enforce desirable but naturally unstable operating conditions. An important example is the efficient suppression of oscillatory vortex shedding, where the feedback mechanisms maintains an amplitude and phase relationship between the actuator and sensor signals (Roussopoulos, 1993), and the response to flow changes happens in fractions of the hydrodynamic time scale. In addition, flow information may be used on longer time scales, to respond to slowly varying flow changes and adapt amplitude and frequency of an otherwise open-loop actuation. In both cases, the coupling between sensors (output) and actuators (input) is based on a mathematical dynamic model which may or may not explicitly resolve the flow structures.

Experimental input-output relationships have been compressed in black-box models without coherent-structure resolution and have proven to be successful in large number of experiments (Becker *et al.*, 2007). Control based on reduced order models for the coherent structures bears the advantage of an enhanced understanding of the actuation and sensing effects relative to the physics of the system (Henning *et al.*, 2006; Pastoor *et al.*, 2006). In addition, Navier-Stokes based nonlinear control strategies may overcome challenges of control design based on linear black-box models (Collis *et al.*, 2004; Noack *et al.*, 2004; Siegel *et al.*, 2003, Tadmor *et al.*, 2004).

Apart from control design, ROMs are also particularly suitable for quick parametric studies. A parametric study of actuation, sensing and control opportunities may become expensive in wind- or water-tunnel as well as with computational fluid dynamics simulations. Hence, reduced models may be useful for less expensive exploration of control opportunities. In addition, closed-loop control in experiment requires robust and online-capable feedback laws. Robustness and simplicity imply sufficiently low-dimensional models, which are accurate enough to resolve the most relevant flow structures and have no "superfluous" degree of freedom (Gerhard *et al.*, 2003; Rowley and Juttijudata, 2005).

The current paper addresses key enablers for least-order models. First (Section 2), the general strategy is outlined. Section 3 recapitulates the standard proper orthogonal decomposition (POD) modeling procedure. In Section 4, missing dynamically important modes in the POD approximations are recapitulated. Sections 5-8 are devoted to 'least-dimensional' Galerkin models for oscillatory processes. A phase-invariant 3-dimensional model for oscillatory fluctuations is derived in Section 5. In Sections 6 and 7, an efficient mode-interpolation method is proposed to account for mode changes kinematically and dynamically in the Galerkin framework. Thus, the dynamic model range is increased at fixed model dimension of 3. In Section 8, this 3-dimensional model is derived only from generalized mean-field considerations without flow input. Finally (Section 9), the main results are summarized.

2. General philosophy of flow control for stabilization

Consider the discrete, linearized Navier-Stokes equation and let the flow velocity field be decomposed into the steady part \mathbf{u}_s and the fluctuation \mathbf{u}'

$$\mathbf{u} = \mathbf{u}_s + \mathbf{u}' \quad (2.1)$$

A general flow control approach can be based on the inclusion of a volume force term in the linearized Navier-Stokes equations

$$\partial_t \mathbf{u}' + \nabla \cdot (\mathbf{u}_s \otimes \mathbf{u}' + \mathbf{u}' \otimes \mathbf{u}_s) = -\nabla p' + \frac{1}{\text{Re}} \Delta \mathbf{u}' + \sum_{l=1}^{N_b} b_l(t) \mathbf{g}_l(\mathbf{x}) \quad (2.2)$$

Any spatial discretization (FDM, FEM, FVM) of (2.2) yields a finite-dimensional evolution equation of the form

$$\frac{d}{dt} \mathbf{a} = \mathbf{A} \mathbf{a} + \mathbf{B} \mathbf{b} \quad (2.3)$$

where \mathbf{a} is a vector of state variables and \mathbf{b} is the actuation command. Sensor measurements are included, in the linear time invariant setting, in the form

$$\mathbf{y} = \mathbf{C}\mathbf{a} \quad (2.4)$$

Using the wake flow behind a circular cylinder as an example, the eigenvalue spectrum of the matrix \mathbf{A} is depicted in Fig. 1. A conjugate pair of eigenvalues in the right-hand side of the complex plane represents the flow instability. Flow control techniques target at the suppression of instability.

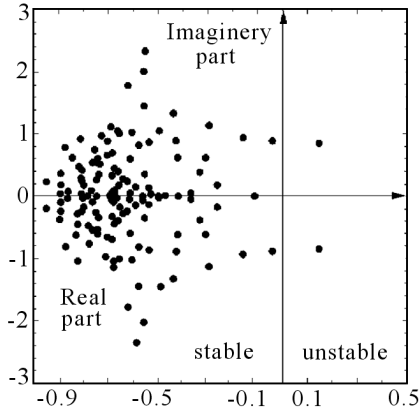


Fig. 1. Eigenvalue spectrum of flow around circular cylinder, $Re = 100$

In terms of the linear equation, suppression of the instability means an effective change of matrix \mathbf{A} , moving the unstable eigenvalues to the left-hand (stable) side of the complex plane. Active proportional controller $\mathbf{b} = \mathbf{K}\mathbf{a}$, for instance, gives rise to the forced dynamics

$$\frac{d}{dt}\mathbf{a} = \mathbf{A}^c\mathbf{a} \quad (2.5)$$

with the modified linear term $\mathbf{A}^c = \mathbf{A} + \mathbf{B}\mathbf{K}$. Here, the design parameter \mathbf{K} may be used to stabilize or destabilize the system and the flow control flow problem can be treated as an extension of the flow stability problem. More generally, in the linear model framework, the sensor signal $\mathbf{y}(t)$ is transferred to actuator signal $\mathbf{b}(t)$ by a feedback controller \mathbf{K} . An example is a PID controller, which may also contain proportional, integral and derivative terms

$$\mathbf{b} = \mathbf{K}_P\mathbf{y} + \mathbf{K}_I \int_0^t \mathbf{y} dt + \mathbf{K}_D \frac{d\mathbf{y}}{dt} \quad (2.6)$$

Depending on the dimension of the vectors \mathbf{b} and \mathbf{y} , one relates to a SISO (single input single output – for one dimension) or MIMO (multiple input multiple output – for higher dimension) control.

The volume force $\mathbf{B}\mathbf{b}$ can represent Lorentz forces or a buoyancy term and can substantially change the solution of the Navier-Stokes equations. It can also mimic the active or passive control devices. For example in the penalty method of CFD, obstacles are modeled by time-dependent volume forces which lead to vanishing velocity in the obstacle. This corresponds to a local actuation term $\mathbf{B}\mathbf{b}$ and a strongly stabilizing controller $\mathbf{b} = \mathbf{K}\mathbf{a}$. Thus, the actuation term of (2.3) may model passive control with control wires, splitter plates, riblets or other devices. Here, \mathbf{A}^c describes the effect of the device and optimization of a passive device may be guided by global stability analysis (Morzyński *et al.*, 2006a). Volume force can also mimic active acoustic actuator (Rowley and Juttijudata, 2005) or wall-mounted actuators (Rediniotis *et al.*, 2002).

Closed-loop control requires model of the flow. Robust closed-loop control can be based on:

- i) high dimensional model described by (2.2)
- ii) low dimensional representation of (2.2)
- iii) experimentally identified black-box models

Approach i) has no practical value in actual applications: real-time control decisions need to be made in milliseconds, ruling out the solution of the Navier-Stokes equations. Black-box controllers iii) are quite successful in some applications (King *et al.*, 2004) but tend to have a limited region of validity. Black-box models are mostly linear and more sophisticated nonlinear models are harder to construct in a black-box framework.

Yet feasible closed-loop performance is determined by the ROM quality. This is illustrated in Fig. 2 showing that while control is based on a higher fidelity, hybrid POD model attenuates the turbulence kinetic energy (TKE) down to about 5% of that of the natural attractor; a controller based on a simpler minimum order POD model enables only partial stabilization.

State feedback, such as $\mathbf{b} = \mathbf{K}\mathbf{a}$ assumes complete access to the state. The reconstruction of the state from sensor measurements necessitates construction of a dynamic observer (Gerhard *et al.*, 2003). In particular, it exploits the knowledge of the system dynamics to derive the complete ROM state from limited sensor information. In evolution equation it is introduced by adding the correction term penalizing the difference between the estimated and measured sensor signal values. As oscillations are attenuated, phase matching becomes difficult (Tadmor *et al.*, 2003) especially when actuation is based on dynamic state estimation.

It is of interest of control the design to derive flow model, smoothly and continuously passing from one operating condition to another. For example, for circular cylinder the operating conditions (Fig. 3) range from the state near the fixed point (steady solution) to the limit cycle (time-averaged flow).

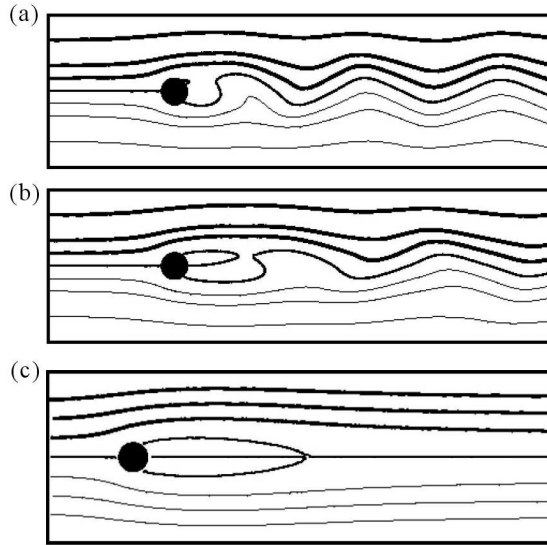


Fig. 2. From top to bottom: natural flow, flow controlled with Galerkin model based actuation with standard POD model, flow controlled with Galerkin model based actuation with hybrid POD model

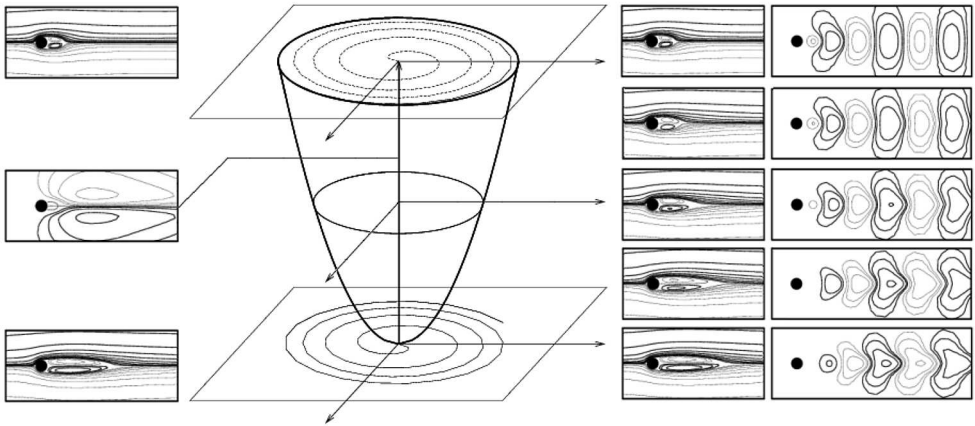


Fig. 3. Principal sketch of the wake dynamics. The left side displays the mean flow (top), shift-mode (middle) and steady solution (bottom). The right side illustrates interpolated vortex streets on the mean-field paraboloid (middle column). The flow mean-fields are depicted also as the streamline plots

While the fixed point operating conditions are precisely described by flow stability eigenmodes with the transition and increased value of the fluctuation amplitude, the modes structure changes up to the one corresponding to oscillatory limit cycle related to the POD modes. In the same time the coherent structures are distorted, the oscillation period and growth rate increases,

and the maximum of the turbulent kinetic energy moves toward the cylinder (Fig. 7). This explains why in the controlled flow situation, the use of POD modes computed for the wrong orbit results in false prediction of the phase of the controller and leads to deterioration of the controlling effect.

3. Empirical Galerkin model

Standard Galerkin method (Fletcher, 1984; Holmes *et al.*, 1998; Ladyzhenskaya, 1963) decomposes the velocity field in a base flow \mathbf{u}_0 and fluctuation \mathbf{u}' . Velocity field is approximated in physical domain Ω with space dependent expansion modes \mathbf{u}_i and time-dependent Fourier coefficients a_i

$$\mathbf{u}^{[0,\dots,N]} = \mathbf{u}_0 + \sum_{j=1}^N \alpha_j \mathbf{u}_j = \sum_{j=0}^N \alpha_j \mathbf{u}_j \quad a_0 \equiv 1 \quad (3.1)$$

Basic mode \mathbf{u}_0 is included in the approximation. The ansatz (3.1) can serve for deriving high-dimensional FEM model (computational Galerkin method) if expansion modes have local compact support on grid cells (FEM's hats). Low-dimensional models and robustness which is our goal in designing the flow model for control purposes, requires traditional Galerkin method which is based on global expansion modes. Traditional Galerkin method (Fletcher, 1984; Holmes *et al.*, 1998; Ladyzhenskaya, 1963) is based on a Hilbert space for the fluctuation $\mathbf{u}' := \mathbf{u} - \mathbf{u}_0$. A typical choice of the Hilbert space is the set of square-integrable solenoidal vector fields $\in \mathcal{L}^2(\Omega)$ with the corresponding inner product between two vectors \mathbf{u}, \mathbf{v}

$$(\mathbf{u}, \mathbf{v})_{\Omega} = \int_{\Omega} \mathbf{u} \cdot \mathbf{v} \, d\mathbf{x} = 0 \quad (3.2)$$

The least-dimensional representation of a single operating condition is obtained with empirical Galerkin method (Cordier and Bergmann, 2003; Holmes *et al.*, 1998). Expansion modes are determined with Karhunen-Loève decomposition (Holmes *et al.*, 1998) (POD) decomposition. Usually the snapshot version (Aubry *et al.*, 1988; Sirovich, 1987) of analysis of the experimental or simulation data is applied. Model based on *a priori* mathematical modes, such as harmonic base functions, typically requires a much larger number of modes for the same, or even lower resolution. Pure physical mode basis obtained with linear stability analysis (Morzyński *et al.*, 1999; Morzyński and Thiele, 1991) of Navier-Stokes equation is adequate for single operating condition and insufficient for representing the flow distant from instability onset. The evolution

equation of the Fourier coefficients is derived from the Galerkin approximation (3.1) by a Galerkin projection of the Navier-Stokes equation onto the expansion modes \mathbf{u}_i (Holmes *et al.*, 1998). The resulting *Galerkin system* has the form

$$\frac{d}{dt}a_i = \nu \sum_{j=0}^N l_{ij}a_j + \sum_{i=0}^N \sum_{j=0}^N q_{ijk}a_ja_k \quad (3.3)$$

where $l_{ij} := (\mathbf{u}_i, \Delta \mathbf{u}_j)_\Omega$ and $q_{ijk} := (\mathbf{u}_i, \nabla \cdot [\mathbf{u}_j \mathbf{u}_k])_\Omega$.

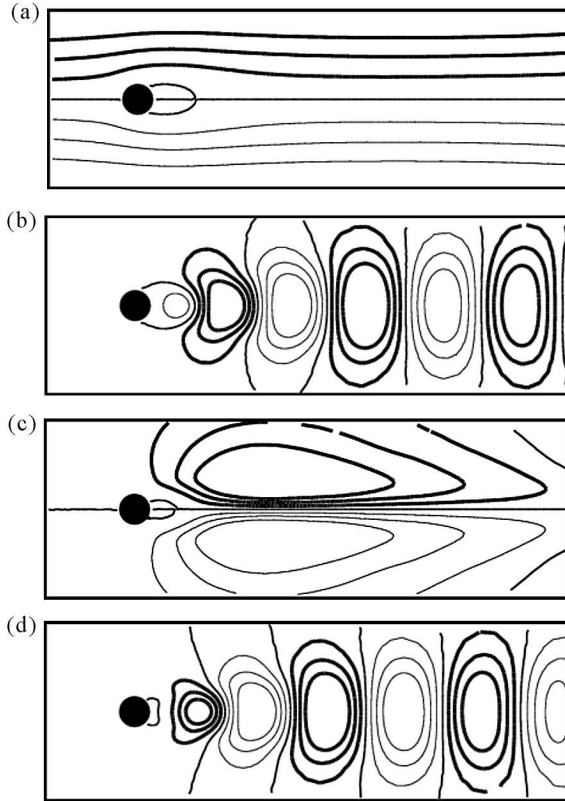


Fig. 4. Streamlines of the mean flow (a), shift mode (c), and first POD modes (b), (d)

Reduced Order Model obtained with the POD Galerkin method is highly efficient and resolves nearly perfectly the kinematics of the flow. At the same time it is highly fragile and sensitive to changes in the parameters or operating conditions. First two POD modes, Fig. 4, of a circular cylinder wake flow for $Re = 100$ capture about 95% of the perturbation energy. It more than sufficient to represent the time evolution of the dominant coherent flow structures, and to determine the phase of the flow for the dissipative feedback control. Yet the Galerkin model, based on these two modes, is structurally unstable. It is

incapable of representing the dynamics of even small perturbations from the attractor, or to predict its amplitude. Six POD modes capture 99.9% TKE but still lead to structurally unstable GM. The inclusion of eight POD modes, capturing the first four harmonics of the attractor, suffices to achieve nearly perfect resolution and structurally stable GS. Yet the correct prediction of dynamics of the system with this model is limited to a small neighborhood of the attractor, and to relatively small Reynolds number perturbations (Deane *et al.*, 1991; Noack *et al.*, 2003).

As can be seen from the quoted examples, the quality of prediction can be improved by increased number of modes. The approach based on a union of modes to extend the dynamic bandwidth of the model is often used. Ma and Karniadakis (2002) add modes of 2D vortex shedding to 20 POD of the 3D flow to resolve the transition from 2D to 3D wake dynamics. The narrow bandwidth of POD-based Galerkin model is even more pronounced for controlled flow and under changing operating conditions. One example of operating condition is the Reynolds number. The deviation from the Reynolds number for which the Galerkin approximation is made results in poor properties of the Galerkin model. Deane *et al.* (1991) showed that the POD modes determined for $Re = 100$ can resolve only 35% of the fluctuation energy at $Re = 150$. Preserving adequate dynamics for model-based MISO control with the use of Galerkin flow model (Bergmann *et al.*, 2005), necessities about 40 POD modes obtained of transient forced data while only 2 POD modes are required for natural flow.

With control-oriented models, significant increase of the number of modes is not possible because the high-dimensional model requires the computational effort comparable with DNS and is useless in online, real life prediction of flow state. The increase of modes basis with single modes is possible but the modes have to be chosen carefully and POD basis is not the optimal choice. The key enabler of ROMs in control-oriented applications is the shift-mode concept (Gerhard *et al.*, 2003; Noack *et al.*, 2003). Further improvement can be obtained with hybrid mode basis (Noack *et al.*, 2003). Continuous mode interpolation is an alternative way of construction of least-dimensional Galerkin approximation.

4. Improvements of Galerkin model

4.1. Mean-field correction: The shift mode

Stabilization of the GM can be obtained with the shift mode (Gerhard *et al.*, 2003; Noack *et al.*, 2003) as suggested by the mean-field theory (Stuart, 1958).

Shift mode is a normalized difference $\mathbf{u}_0 - \mathbf{u}_s$ where \mathbf{u}_0 is the mean flow solution and \mathbf{u}_s is the (unstable) steady solution. Examples of the stabilizing effect of mean field corrections are shown also by Siegel *et al.* (2003), Zielinska and Wesfreid (1995).

The inclusion of the shift mode reduces model sensitivity to parameter variations and is an enabler for the low-dimensional representation of transient manifolds, such as the one connecting the unstable steady solution to the attractor. The dynamics of the minimum Galerkin Model with a shift mode is compared with DNS in Fig. 5 and Fig. 6. Shift mode is the key enabler for construction of transient, control-oriented models.

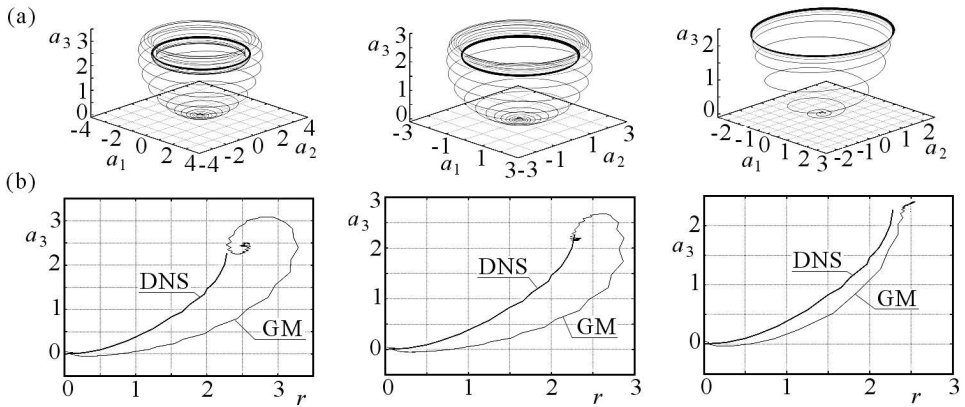


Fig. 5. Galerkin model with shift-mode and 2 POD modes (left), 8 POD modes (middle) and continuous mode interpolation (2 modes); (a) dynamics of the first three Fourier coefficients of the Galerkin model, (b) mismatch between direct numerical simulation (DNS) and Galerkin system; transients of a_3 as a function of r

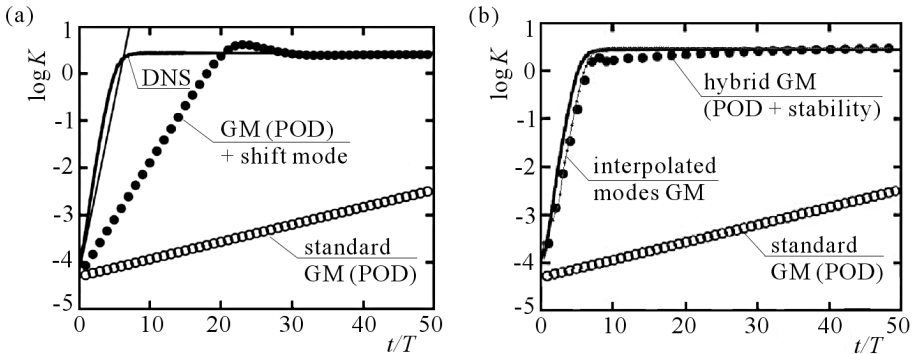


Fig. 6. Transients of Galerkin models; (a) traditional POD-based models, (b) improvement of GM dynamics – hybrid model and continuous mode interpolation

4.2. Hybrid model employing stability modes

Different shape of the wake structures at the onset of instability and at the limit cycle precludes a uniformly accurate minimal Galerkin model for the entire transient, from steady to the periodic solution. While the Galerkin model based on Karhunen-Loève modes predict much better the fluctuation near the limit cycle, the one employing two stability eigenmodes properly describes the vicinity of steady solution. In order to combine the strength of the both models a hybrid model is constructed with two KL modes, two stability modes and the shift-mode.

In this model POD resolve the attractor and stability eigenmodes resolve the linearized dynamics. Thus, dynamic transient and post-transient flow behavior was accurately predicted. The concept of hybrid model reduces significantly the number of necessary degrees of freedom of the system. The transients of the hybrid models are compared with DNS in Fig. 6. The hybrid model combines the advantages of both reduced models. It converges to the limit cycle preserving initially the growth rate predicted by global stability analysis.

5. Phase-invariant Galerkin flow model

Galerkin system for dominant oscillatory flow dynamics may be nearly independent of the oscillation phase. The independence of phase for the control-oriented model can be obtained without noticeable loss of accuracy by phase averaging of the Galerkin system. The phase of the model θ is determined by the angle between a_1 and a_2 , $\theta = \arctan(a_1/a_2)$. In the phase-invariant model the coefficients l_{ij} and q_{ijk} in (3.3) must remain constant for any rotation of the coordinate system. Rotation of the space span by Fourier coefficients (vector) around a_3 axis by the angle of θ is given by

$$\begin{bmatrix} 1 \\ a_1 \\ a_2 \\ a_3 \end{bmatrix} = \begin{bmatrix} 1 & 0 & 0 & 0 \\ 0 & \cos \theta & \sin \theta & 0 \\ 0 & -\sin \theta & \cos \theta & 0 \\ 0 & 0 & 0 & 1 \end{bmatrix} \begin{bmatrix} 1 \\ a_1^\theta \\ a_2^\theta \\ a_3^\theta \end{bmatrix} \tag{5.1}$$

We assume that

$$a_1 = A \sin(\omega t) \qquad a_2 = A \cos(\omega t) \tag{5.2}$$

If the desired system is phase-invariant (independent of θ), the coefficients of "rotated" and original system must be the same as the original one

$$l_{ij}^\theta = l_{ij} \qquad q_{ijk}^\theta = q_{ijk} \tag{5.3}$$

Coefficients l_{ij}^θ and q_{ijk}^θ resulting from rotation (5.1) are given by

$$l_{ij}^\theta = \sum_{l=1}^3 \sum_{m=0}^3 T_{li} l_{lm} T_{mj} \quad (5.4)$$

$$q_{ijk}^\theta = \sum_{l=1}^3 \sum_{m=0}^3 \sum_{n=0}^3 T_{li} q_{lmn} T_{mj} T_{nk}$$

Further we average in time all the coefficients

$$l_{ij}^* = \frac{1}{2\pi} \int_0^{2\pi} l_{ij}^\theta d\theta \quad (5.5)$$

$$q_{ijk}^* = \frac{1}{2\pi} \int_0^{2\pi} q_{ijk}^\theta d\theta$$

With this operation, many of the coefficients are vanishing due to presence of functions sin and cos under the integral.

The resulting phase-invariant system reads

$$\begin{aligned} \dot{a}_1 &= (\sigma_r - \beta a_3) a_1 + (\omega + \gamma a_3) a_2 \\ \dot{a}_2 &= (\sigma_r - \beta a_3) a_2 - (\omega + \gamma a_3) a_1 \\ \dot{a}_3 &= -\sigma_\Delta a_3 + \delta_0 + \delta_2 a_3^2 + \alpha(a_1^2 + a_2^2) \end{aligned} \quad (5.6)$$

where σ_r , β , ω , γ , σ_Δ , δ_0 , δ_2 are computed with (non-zero) l_{ij} and q_{ijk} . It should be noted that now the system is described only by 6 parameters, in comparison to 60 parameters of the original one.

We now want to formulate our phase-invariant Galerkin model in terms of amplitude r , phase θ and shift mode amplitude $a_\Delta = a_3$. With $r^2(t) = a_1^2(t) + a_2^2(t)$ and $\theta = \arctan(a_1/a_2)$, the time derivative of the equation $r^2(t) = a_1^2(t) + a_2^2(t)$ is

$$2r\dot{r} = 2a_1\dot{a}_1 + 2a_2\dot{a}_2 \quad (5.7)$$

The phase angle derivative $\dot{\theta}$ is given by

$$\dot{\theta} = \frac{a_2\dot{a}_1 - a_1\dot{a}_2}{a_1^2 + a_2^2} \quad (5.8)$$

so our phase-invariant model in polar coordinates can be written

$$\begin{aligned} \dot{r} &= (\sigma_r - \beta a_\Delta) r & \dot{\theta} &= \omega + \gamma a_\Delta \\ \dot{a}_\Delta &= -\sigma_\Delta a_\Delta + \delta_0 + \delta_2 a_\Delta^2 + \alpha r^2 \end{aligned} \quad (5.9)$$

If we assume small amplitude of a_Δ and take into account that δ_0 can be set to zero for steady flow base solution \mathbf{u}_0 , the equations further simplifies. Additionally we can assume slow variation in time of a_Δ , so $\dot{a}_\Delta = 0$ and the third equation reduces to algebraic expression for a_Δ as a function of r

$$a_\Delta = \frac{\alpha}{\sigma_\Delta} r^2 \tag{5.10}$$

Post-transient solution of the system (5.6) reads

$$a_1 = A \sin(\omega t) \qquad a_2 = A \cos(\omega t) \qquad a_\Delta = B \tag{5.11}$$

The transients can be described by the Kryloff-Bogoliubov ansatz allowing for slow variation of the amplitudes A , B and frequency ω in time.

Actuation in (5.6) can be mimicked with the right-hand side volume force. Considering, for example, actuation with transverse oscillation of the cylinder (Tadmor *et al.*, 2004) the model (5.6) reads

$$\begin{bmatrix} \dot{a}_1 \\ \dot{a}_2 \\ \dot{a}_3 \end{bmatrix} = \begin{bmatrix} \sigma_r & -(\omega + \gamma a_3) & -\beta a_1 \\ (\omega + \gamma a_3) & \sigma_r & -\beta a_2 \\ \alpha a_1 & \alpha a_2 & -\sigma_\Delta \end{bmatrix} \begin{bmatrix} a_1 \\ a_2 \\ a_3 \end{bmatrix} + \begin{bmatrix} g_1 \\ g_2 \\ 0 \end{bmatrix} \Gamma \tag{5.12}$$

where g_1, g_2 are new coefficients and $\Gamma = -\ddot{y}_{cyl} = \dot{a}_c$. Here a_c denotes amplitude of the actuation mode. Different control strategies can be tested with this model as presented by Gerhard *et al.* (2003), Noack *et al.* (2004), Tadmor *et al.* (2004).

6. Interpolated modes

The "ideal" set of modes should not only adequately represent the flow dynamics and transients but also "adapt itself" to the controlled flow conditions. The idea of mode parameterization instead of increasing the number of POD modes is pursued by several groups. Luchtenburg *et al.* (2006) employ a parameterization based on control. Further improvement of the Galerkin model for control purposes is presented in Lehmann *et al.* (2005). The POD modes are derived from the controlled flow subjected to moderate or aggressive forcing. In this way the dominant modes change along the transients is taken into account. The concept of interpolated POD modes used for circular cylinder flow control is elaborated in details in Lehmann *et al.* (2005). While retaining relatively large number of modes (about 40) only 3 Fourier coefficients have to be dynamically estimated in the controller. Siegel *et al.* (2006) employ short

time sampling of transient flows to improve the dynamical properties of the model.

In Morzyński *et al.* (2006a,b) a novel continuous mode interpolation technique is proposed. The mode interpolation smoothly connects not only different operating conditions, but also stability and POD modes. In addition, the extrapolation of modes outside the design conditions is possible. Interpolated modes enable the 'least-order' Galerkin models keeping the dimension from a single operating condition but resolving several states. These models are especially well suited for control design.

To demonstrate the continuous mode interpolation we assume that \mathbf{A}_o is a linearized Navier-Stokes operator or the FEM discretization as stability matrix. A linear interpolation of the underlying eigenproblems can be performed with κ as the interpolation parameter. Here, $\kappa = 0$ for the steady flow and stability eigenmodes, and $\kappa = 1$ for the periodic flow and POD modes.

The simplest form of local linearization can be obtained by linear interpolation of matrices \mathbf{A}_o and \mathbf{A}_s at two different states

$$\mathbf{A}(\kappa) = \mathbf{A}_s + \kappa(\mathbf{A}_o - \mathbf{A}_s) \quad (6.1)$$

The \mathbf{A}_s matrix refers to the steady flow conditions and \mathbf{A}_o – to the periodic limit cycle.

In practice this technique is adequate only for mode interpolation of the same basis. The stability matrix with non-normal eigenvectors and complex eigenvalues requires special treatment to be interpolated with symmetric Fredholm kernel, hermitian eigenvalue problem with real eigenvalues. Details of this procedure can be found in Morzyński *et al.* (2006a).

6.1. Interpolation between POD and stability eigenmode basis

The method presented in Section 6 is tested in Morzyński *et al.* (2006a,b) on interpolation of the POD and stability eigenmode basis. For practical control applications, more important than simple linear interpolation between bases of the same mode is a more complex problem of different mode basis.

Fig. 7 shows the results of the corresponding interpolated modes \mathbf{u}_i^κ . The detail results can be found in Morzyński *et al.* (2006a).

For interpolation, the real part of the most unstable stability mode and the first POD mode is applied. Interpolation, performed for the wake behind a circular cylinder at $\text{Re} = 100$, is shown in Fig. 7. The modes change smoothly from one operating state to another. Thereby, the maximum of fluctuation level moves to the outflow. A similar observation has been made by Lehmann *et al.* (2005) for the flow subjected to increasingly aggressive stabilizing control.

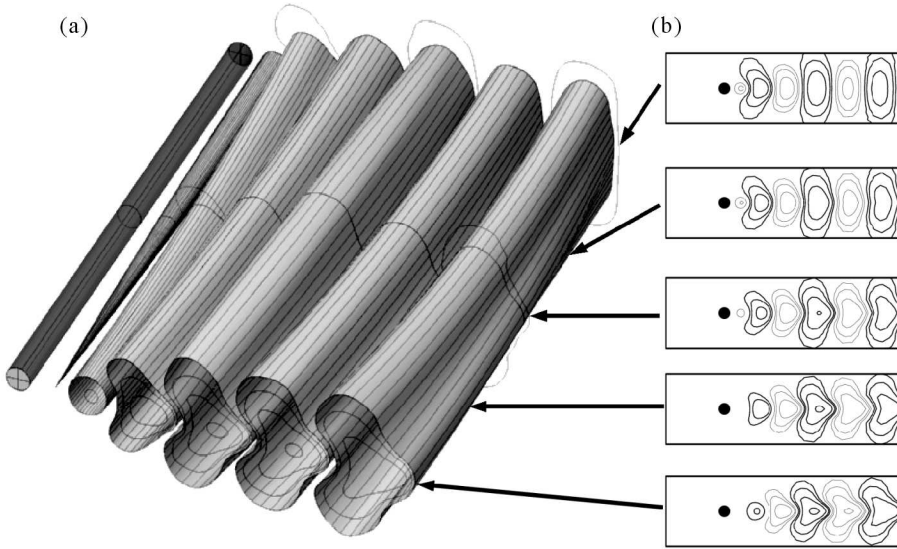


Fig. 7. Interpolated modes; (a) streamlines of the mode continuously changing with κ , (b) interpolated modes for $\kappa = 1.0$ (the most energetic POD mode), $\kappa = 0.75$, $\kappa = 0.50$ and $\kappa = 0.25$, $\kappa = 0$ (real part of the dominant eigenvector)

7. Galerkin models based on interpolated modes

7.1. General methodology

Adopting the concept of continuous mode interpolation, the low-dimensional Galerkin model can be derived in a straightforward manner (Noack *et al.*, 2005) assuming a slowly varying κ

$$\frac{d}{dt}a_i^\kappa = \frac{1}{\text{Re}} \sum_{j=0}^N l_{ij}^\kappa a_j^\kappa + \sum_{j,k=0}^N q_{ijk}^\kappa a_j^\kappa a_k^\kappa + \sum_{l=1}^{N_b} g_{il}^\kappa b_l \tag{7.1}$$

$$\frac{d}{dt}\kappa = F(\kappa, \mathbf{a}^\kappa, \mathbf{b})$$

The Galerkin system coefficients l_{ij}^κ and q_{ijk}^κ depend on the operating condition κ . During a natural transient of an oscillatory flow, \mathbf{u}_0^κ may be the phase-averaged velocity and κ may be identified with the shift-mode amplitude (Noack *et al.*, 2003). Moreover, (7.1)₂ is derived from the Navier-Stokes equation filtered with the phase average $\langle \cdot \rangle$ and projected onto the mean-field correction. During an actuated transient, κ may be identified with a forcing amplitude or frequency. In this case, (7.1)₂ is replaced by a prescribed dynamics of κ .

In a simple case, the Galerkin system coefficients may be linearly interpolated between two closely operating conditions identified by $\kappa = 0$ and $\kappa = 1$

$$\begin{aligned} l_{ij}^\kappa &= l_{ij}^0 + \kappa(l_{ij}^1 - l_{ij}^0) \\ q_{ijk}^\kappa &= q_{ijk}^0 + \kappa(q_{ijk}^1 - q_{ijk}^0) \end{aligned} \quad (7.2)$$

Model (7.1) targets the least-dimensional representation of the flow. With only two interpolated modes, shift mode and the parameter κ , the flow is represented in the very wide range of significantly different operating conditions. From the point of view of the flow control practice, this is of the highest importance.

In the same time the described method can be a crucial step toward construction of the fully *a priori* model of the time-averaged flow, based only on the steady solution of the Navier-Stokes equations and physical stability eigenmodes.

7.2. Least-dimensional model for oscillatory flows

In this section, the Galerkin model based on continuously interpolated modes (described in Section 7.1) is presented and compared with the commonly used POD Galerkin models and DNS.

In the model two mode sets are included. For the state corresponding to the fixed point, the two most unstable eigenmodes of global stability analysis are used. For limit cycle dynamics, two first POD modes have been chosen. Base flow and shift mode remain unchanged, while two remaining modes depend on the operating conditions.

In Galerkin model, constructed as in (7.1), the interpolation parameter κ is identified with shift-mode amplitude a_3

$$\kappa = \frac{a_3}{a_3^\bullet} - 1 \quad (7.3)$$

where a_3^\bullet represents amplitude of the shift mode for periodic solution. In this way κ changes continuously, allowing proper interpolation of the used modes and Galerkin system coefficients (7.1)₂. Since the interpolated modes are matching the transients of the flow better than POD modes, the dynamical behavior of minimum model based on interpolated modes (represented in Fig. 6 by the turbulent kinetic energy of fluctuation K) is much closer to DNS results than in case of POD-only models.

Presented model, containing only 3 degrees of freedom (two interpolated modes and shift-mode), is more accurate than the 7-dimensional POD model (Fig. 5 and Fig. 6).

8. *A priori* model of the flow

A major step towards *a priori* flow model would be prediction of POD modes on the basis of stability eigenmodes. Global flow stability analysis predicts exactly the periodic flow behavior near the fixed point, only with the steady base flow. Composition of this predictive feature with continuous mode interpolation should accomplish the desired solution.

In Fig.8 extrapolation of physical modes to approximate empirical ones is shown. Starting points are eigenmodes computed from a global stability analysis of the steady solution and of time-averaged flow. The POD mode shall be expressed in terms of these physical modes (stability eigenmodes) only.

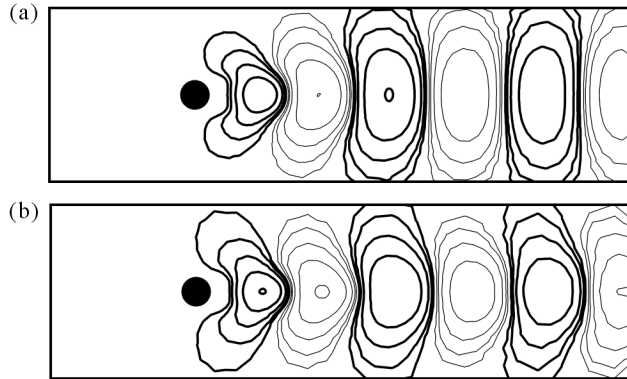


Fig. 8. Computed (a) and approximated on the basis of stability eigenmodes (b) POD mode for $Re = 100$

In Fig.9 the flow field reconstructed with the use of extrapolated POD mode is shown. In the near wake it is close to the one based on POD modes. As the near wake is particularly important for flow control, the results of the *a priori* mode interpolation are encouraging.

9. Conclusions

In the current study, reduced order modeling for control design is discussed and exemplified for the cylinder wake. Starting point is the standard POD Galerkin model utilizing its low dimension by construction. The price for low dimension is an over-optimization for a single reference condition, i.e. a small dynamic bandwidth. This dynamic bandwidth is significantly increased by additional expansion modes provided by mean-field considerations. A hybrid

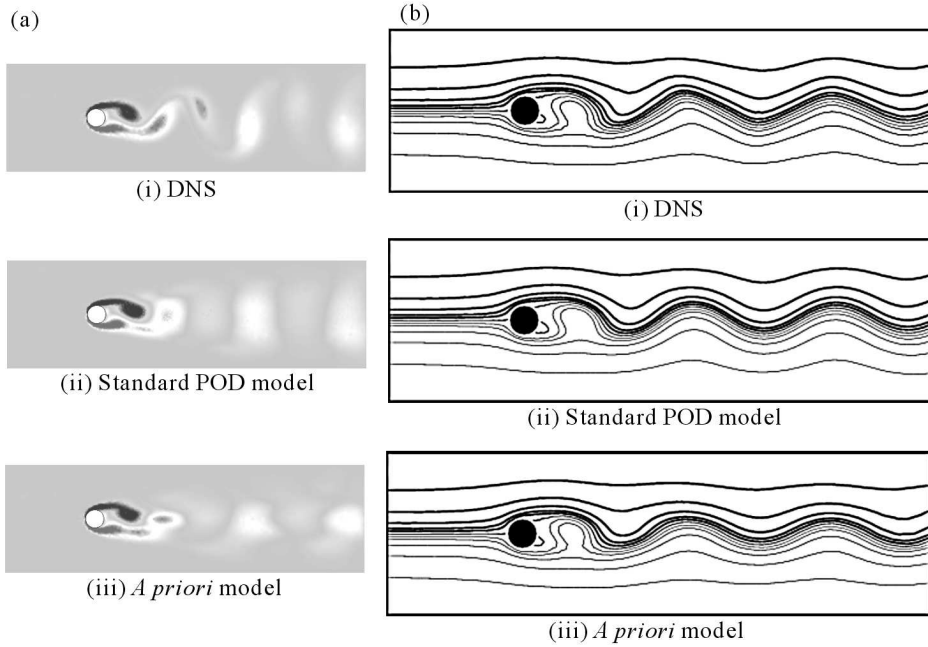


Fig. 9. *A priori* Galerkin model based on flow stability eigenmodes. Vorticity (a) and streamlines (b) are depicted for $Re = 100$

model with 8 POD modes and 3 mean-field modes describes well the transient from the steady to periodic flow.

The order of the hybrid model can be significantly reduced, realizing that transient oscillatory fluctuations may be resolved by 2 base-flow dependent modes. The deformation between stability eigenmodes near the steady solution and 2 POD modes for the limit cycle dynamics, is resolved by a novel continuous mode interpolation technique. Thus, a 3-dimensional 'least-order' model is constructed which has an accuracy comparable to the 11-dimensional hybrid model, but has a significantly increased robustness. Intriguingly, continuous mode interpolation can be employed for interpolation and extrapolation between modes at different Reynolds numbers, angle of attack, and other parametric changes.

In the final step, an *a priori* generalized mean-field model is constructed in which all modes are derived from the stability analysis, from the Reynolds equation and from the continuous mode interpolation. In particular, the shift mode and the POD are approximated from Navier-Stokes considerations without the need for empirical input. The authors currently pursue applications of this generalized mean-field models for control design, including multi-frequency physics.

Acknowledgments

The work has been funded by the Deutsche Forschungsgemeinschaft (DFG) under grants No. 258/1-1 and No. 258/2-3, by the US National Science Foundation (NSF) under grants 0524070 and 0410246, and by the US Air Force Office of Scientific Research (AFOSR) under grants FA95500510399 and FA95500610373. The authors acknowledge funding and excellent working conditions of the Collaborative Research Center (Sfb 557) "Control of complex turbulent flow" which is supported by the DFG and hosted at the Technical University Berlin. Stimulating discussions with Eckart Meiburg, Michael Schlegel, Jon Scouten and Tino Weinkauff are acknowledged. We are grateful for outstanding hardware and software support by Lars Oergel and Martin Franke at TU Berlin.

References

1. AUBRY N., HOLMES P., LUMLEY J.L., STONE E., 1988, The dynamics of coherent structures in the wall region of a turbulent boundary layer, *J. Fluid Mech.*, **192**, 115-173
2. BECHERT D.W., BRUSE M., HAGE W., VAN DER HOEVEN J.G.T., HOPPE G., 1997, Experiments on drag-reducing surfaces and their optimization with an adjustable geometry, *J. Fluid Mech.*, **338**, 59-87
3. BECHERT D.W., HOPPE G., 1985, On the drag reduction of the shark skin, *AIAA-Paper 1985-0546*
4. BECKER R., KING R., PETZ W., NITSCHKE W., 2007, Adaptive closed-loop separation control on a high-lift configuration using extremum seeking, *AIAA Journal*
5. BERGMANN M., CORDIER L., BRANCHER J.-P., 2005, Optimal rotary control of the cylinder wake using proper orthogonal decomposition reduced order model, *Phys. Fluids*, **17**, 097101-097121
6. COLLIS S., JOSLIN R., SEIFERT A., THEOFILIS V., 2004, Issues in active control: theory, control, simulation and experiment, *Progress in Aerospace Sciences*, **40**, 237-289
7. CORDIER L., BERGMANN M., 2003, *Proper Orthogonal Decomposition: An Overview*, VKI Lecture Series 2003-04, Von Kármán Institut for Fluid Dynamics
8. DEANE A.E., KEVREKIDIS I.G., KARNIADAKIS G.E., ORSZAG S.A., 1991, Low-dimensional models for complex geometry flows: Application to grooved channels and circular cylinders, *Phys. Fluids A*, **3**, 10, 2337-2354
9. FIEDLER H.-H., FERNHOLZ H., 1990, On the management and control of turbulent shear flows, *Progr. Aeronaut. Sci.*, **27**, 305-387

10. FLETCHER C.A.J., 1984, *Computational Galerkin Methods*, Springer, New York
11. GAD-EL-HAK M., 2000, *Flow Control: Passive, Active and Reactive Flow Management*, Cambridge University Press
12. GAD-EL-HAK M., BUSHNELL D., 1991, Status and outlook of flow separation control, *29th AIAA Aerospace Sciences Meeting*, Reno, Nevada, also as *AIAA-91-0037 Paper*
13. GERHARD J., PASTOOR M., KING R., NOACK B.R., DILLMANN A., MORZYŃSKI M., TADMOR G., 2003, Model-based control of vortex shedding using low-dimensional Galerkin models, *33rd AIAA Fluids Conference and Exhibit*, Orlando, Florida, USA, *Paper 2003-4262*
14. HENNING L., PASTOOR M., KING R., NOACK G., TADMOR B.R., 2006, Feedback control applied to bluff body wake, In: *Notes on Numerical Fluid Mechanics and Multidisciplinary Design (NNFM)*, R. King (Edit.), Springer, Conference on Active Flow Control 2006, Berlin, Germany
15. HOLMES P., LUMLEY J.L., BERKOOZ G., 1998, *Turbulence, Coherent Structures, Dynamical Systems and Symmetry*, Cambridge University Press, Cambridge
16. KIM J.-H., UTKIN Y., ADAMOVICH I., SAMIMY M., 2005, Active control of high speed and high Reynolds numbers jets via plasma actuators, *58th Annual Meeting of the Division of Fluid Dynamics of the American Physical Society, 2005*, *Bulletin Am. Phys. Soc.*, **50**, 9, KT.00004
17. KING R., BECKER R., GARWON M., HENNING L., 2004, Robust and adaptive closed-loop control of separated shear flows, *2nd AIAA Flow Control Conference*, Portland, Oregon, USA, *Paper 2004-2519*
18. LADYZHENSKAYA O.A., 2003, *The Mathematical Theory of Viscous Incompressible Flow*, Gordon and Breach, New York, London
19. LEHMANN O., LUCHTENBURG M., NOACK B.R., KING R., MORZYŃSKI M., TADMOR G., 2005, Wake stabilization using pod galerkin models with interpolated modes, *44th IEEE Conference on Decision and Control and European Control Conference ECC 2005*, Seville, Spain, *Invited Paper 1608*
20. LUCHTENBURG D.M., TADMOR G., LEHMANN O., NOACK B.R., KING R., MORZYŃSKI M., 2006, Tuned POD Galerkin models for transient feedback regulation of the cylinder wake, *44th AIAA Aerospace Sciences Meeting and Exhibit*, Reno, Nevada, USA, *AIAA-Paper 2006-1407J.-P.*
21. LUMLEY J.L., BLOSSEY P.N., 1998, Control of turbulence, *Ann. Rev. Fluid Mech.*, **30**, 311-327
22. MA X., KARNIADAKIS G.E., 2002, A low-dimensional model for simulating three-dimensional cylinder flow, *J. Fluid Mech.*, **458**, 181-190
23. MORZYŃSKI M., AFANASIEV K., THIELE F., 1999, Solution of the eigenvalue problems resulting from global non-parallel flow stability analysis, *Comput. Meth. Appl. Mech. Eng.*, **169**, 161-176

24. MORZYŃSKI M., STANKIEWICZ W., NOACK B.R., KING R., THIELE F., TADMOR G., 2006a, Continuous mode interpolation for control-oriented models of fluid flow, *Notes on Numerical Fluid Mechanics and Multidisciplinary Design (NNFM)*, R. King (Edit.), Springer, Conference on Active Flow Control 2006, Berlin, Germany
25. MORZYŃSKI M., STANKIEWICZ W., NOACK B.R., THIELE F., TADMOR G., 2006b, Generalized mean-field model with continuous mode interpolation for flow control, *3rd AIAA Flow Control Conference*, San Francisco, Ca, USA, *AIAA-Paper 2006-3488*
26. MORZYŃSKI M., THIELE F., 1991, Numerical stability analysis of a flow about a cylinder, *Z. Angew. Math. Mech.*, **71**, T424-T428
27. NOACK B.R., AFANASIEV K., MORZYŃSKI M., TADMOR G., THIELE F., 2003, A hierarchy of low-dimensional models for the transient and post-transient cylinder wake, *J. Fluid Mech.*, **497**, 335-363
28. NOACK B.R., PAPAS P., MONKEWITZ P.A., 2005, The need for a pressure-term representation in empirical Galerkin models of incompressible shear flows, *J. Fluid Mech.*, **523**, 339-365
29. NOACK B.R., TADMOR G., MORZYŃSKI M., 2004, Low-dimensional models for feedback flow control. Part I: Empirical Galerkin models, *2nd AIAA Flow Control Conference*, Portland, Oregon, USA, *AIAA Paper 2004-2408* (invited contribution)
30. PASTOOR M., NOACK B.R., KING R., TADMOR G., 2006, Spatiotemporal waveform observers and feedback in shear layer control, *44th AIAA Aerospace Sciences Meeting and Exhibit*, Reno, Nevada, USA, *AIAA-Paper 2006-1402*
31. REDINIOTIS O.K., KO J., KURDILA A.J., 2002, Reduced order nonlinear Navier-Stokes models for synthetic jets, *J. Fluids Eng.*, **124**, 2, 433-443
32. ROUSSOPOULOS K., 1993, Feedback control of vortex shedding at low Reynolds numbers, *J. Fluid Mech.*, **248**, 267-296
33. ROWLEY C., JUTTIJUDATA V., 2005, Control and estimation of oscillating cavity flows, *57th Annual Meeting of the Division of Fluid Dynamics of the American Physical Society, 2004, Bulletin Am. Phys. Soc.*, **49**, 9
34. SIEGEL S., COHEN K., MCLAUGHLIN T., 2003, Feedback control of a circular cylinder wake in experiment and simulation, *33rd AIAA Fluids Conference and Exhibit*, Orlando, Florida, USA, *Paper No 2003-3571*
35. SIEGEL S., COHEN K., SEIGEL J., MCLAUGHLIN T., 2006, Proper orthogonal decomposition snapshot selection for state estimation of feedback controlled flows, *AIAA Aerospace Sciences Meeting and Exhibit*, Reno/NV, *Paper 2006-1400*
36. SIROVICH L., 1987, Turbulence and the dynamics of coherent structures, Part I: Coherent structures, *Quart. Appl. Math.*, **XLV**, 561-571

37. SMITH A.C., BAILLIEUL J., 2000, Vortex models for the control of flows, *39th IEEE Conference on Decision and Control 2000*, Sydney, Australia, Paper INV 4903
38. SMITH D., AMITAY M., KIBENS V., PAREKH D., GLEZER A., 1998, Modification of lifting body aerodynamics using synthetic jet actuators, *AIAA-Paper 1998-0209*
39. STUART J.T., 1958, On the non-linear mechanics of hydrodynamic stability, *J. Fluid Mech.*, **4**, 1-21
40. TADMOR G., NOACK B.R., DILLMANN A., GERHARD J., PASTOOR M., KING R., MORZYŃSKI M., 2003, Control, observation and energy regulation of wake flow instabilities, *42nd IEEE Conference on Decision and Control 2003*, Maui, HI, USA, 2334-2339, *WeM10-4*
41. TADMOR G., NOACK B.R., MORZYŃSKI M., SIEGEL S., 2004, Low-dimensional models for feedback flow control. Part II: Controller design and dynamic estimation, *2nd AIAA Flow Control Conference*, Portland, Oregon, USA, *AIAA Paper 2004-2409* (invited contribution)
42. THOMAS F., KOZLOV A., CORKE T., 2006, Plasma actuators for bluff body flow control, *AIAA-Paper 2006-2846*
43. WYGNANSKI I., SEIFERT A., 1994, The control of separation by periodic oscillations, *18th AIAA Aerospace Ground Testing Conference*, Colorado Springs, CO, *AIAA-94-2608 Paper*
44. ZIELINSKA B.J.A., WESFREID J.E., 1995, On the spatial structure of global modes in wake flow, *Phys. Fluids*, **7**, 6, 1418-1424

Globalna analiza stabilności i modelowanie niskowymiarowe w zastosowaniu do sterowania opływem ciał

Streszczenie

W pracy przedstawiono grupę modeli niskowymiarowych przeznaczoną do sterowania opływem ciał. Wymagania dotyczące modelu, takie jak prostota, dokładność i odporność wymagają ograniczenia liczby wymiarów. Standardowe modele Galerkina oparte o mody POD okazują się nieprzydatne do projektowania kontrolera, stąd jako rozwiązanie problemu zaproponowano modele hybrydowe oparte o mody globalnej analizy stabilności, mody POD i mod przesunięcia. Dodatkowo zaprezentowano nową koncepcję interpolacji modów, przez co możliwa jest konstrukcja parametrycznego modelu przepływu charakteryzującego się najmniejszą z możliwych liczbą wymiarów i płynną zmianą w zależności od stanu sterowanego przepływu. Metoda ciągłej interpolacji modów została zastosowana do konstrukcji modelu *a priori* przepływu, opartego jedynie o mody globalnej analizy stabilności.